



Groundwater resources in the Kouris catchment (Cyprus): data analysis and numerical modelling

Anastasia Boronina^{a,*}, Philippe Renard^{a,1}, Werner Balderer^{a,2},
Andreas Christodoulides^{b,3}

^a*Institute of Engineering Geology, ETH-Hoenggerberg, Zürich, CH-8093, Switzerland*

^b*Water Development Department of Cyprus, Nicosia, Cyprus*

Received 30 January 2002; revised 10 October 2002; accepted 11 October 2002

Abstract

The Kouris catchment in Cyprus is currently experiencing a scarcity of water resources due to the semi-arid climate across the southern part of the region, a series of dry years, and recent surface/subsurface water over-extraction. The catchment consists of the upper part of an ophiolitic complex in the North, which is considered a very significant aquifer for Cyprus, and an overlying sedimentary complex in the South, which has low water storage capacity.

Water balance calculations are conducted using a steady state groundwater model. The recharge rate was calculated to be between 12 and 16% of the total annual rainfall. This agrees, with an estimate based on the mass balance of chloride. When the rate of extraction was increased to a value close to the present water demand, river baseflow was reduced from 25 to 18 Mm³ per year. Other negative impacts were extreme drawdowns and drying up of springs.

© 2002 Elsevier Science B.V. All rights reserved.

Keywords: Ophiolites; Water management; Semi-arid climate; Cyprus; Mountainous region; Recharge

1. Introduction

The Kouris catchment encompasses an area of 300 km² and extends from the southern side of the Troodos Massif of Cyprus to the Mediterranean Sea

(Fig. 1). The topography is typical of a mountainous area with steep valleys, and surface elevations drop within 30 km from 2000 m in the North to sea level in the South (Fig. 2).

The River Kouris, which drains the catchment (Fig. 3), is the largest in Cyprus and has had an average annual streamflow of 36 Mm³/year during the last 30 years. The Kouris downstream reservoir (Kouris Dam) has the highest storage capacity in Cyprus (110 Mm³), but it has never been filled to the planned level and has stayed almost empty during the years 1998–2000. At the same time, a drop of groundwater levels in the vicinity of irrigation boreholes located in the upper part of the catchment was

* Corresponding author. Tel.: +41-1-633-37-36; fax: +41-1-633-11-08.

E-mail addresses: boronina@erdw.ethz.ch (A. Boronina), philippe.renard@unine.ch (P. Renard), Balderer@erdw.ethz.ch (W. Balderer), ac101246@cytanet.com.cy (A. Christodoulides).

¹ Present address: Centre of Hydrogeology, University of Neuchâtel, Tel.: +41-32-718-26-90; fax: +41-32-718-26-03.

² Tel.: +41-1-633-27-43; fax: +41-1-633-11-08.

³ Tel.: +357-2-304-290.

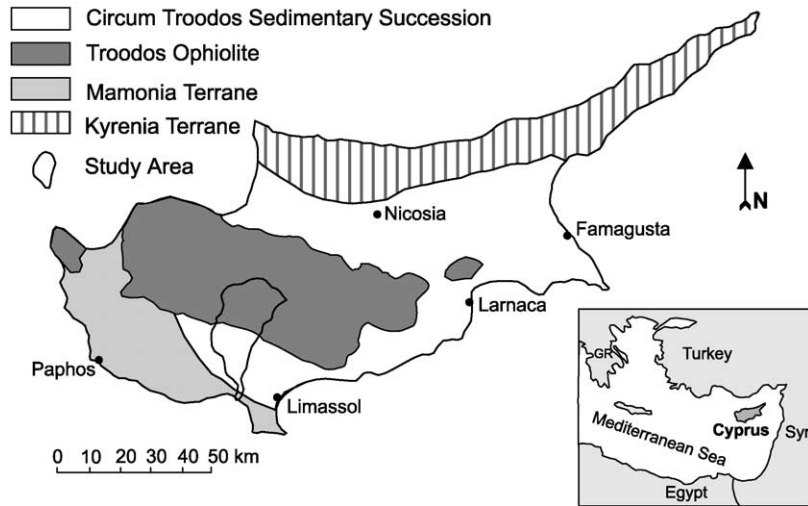


Fig. 1. Simplified geological map of Cyprus showing the location of the Kouris catchment.

observed (Fig. 4). Water conflicts appearing in the catchment motivated the investigations reported in this paper.

The major groundwater resources are associated with the ophiolitic complex, which comprises harzburgites, gabbros, sheeted dykes, and pillow lavas. It is characterised by strong heterogeneity in hydraulic conductivity and porosity related to tectonic fracturing and hydrothermal alteration. The climate is characterised by very high spatial and temporal variability.

There are many scientific publications related to the geology of the Troodos Mountains (Gass et al., 1994; Malpas et al., 1990; van Everdingen, 1995; Gillis and Sapp, 1997; Varga et al., 1999). However, there are no published results related to groundwater occurrence in these ophiolites even though the hydrogeology of the ophiolites was studied in the 70s and 80s and described in several technical reports (Jacovides, 1979; Afrodisis et al., 1986). In the 1980s, most groundwater studies in Cyprus were concerned with isotope investigations (^{18}O , ^2H , ^3H , ^{14}C) (Jacovides, 1979; Verhagen et al., 1991). The area studied included the part of ophiolites of the Kouris catchment. Other studies of the sedimentary complex of Cyprus have focused on estimating recharge from precipitation (Kitching et al., 1980) and the practice of artificial recharge (Jacovides, 1997). The LIFE project (Charalambides et al., 1998) assessed existing and

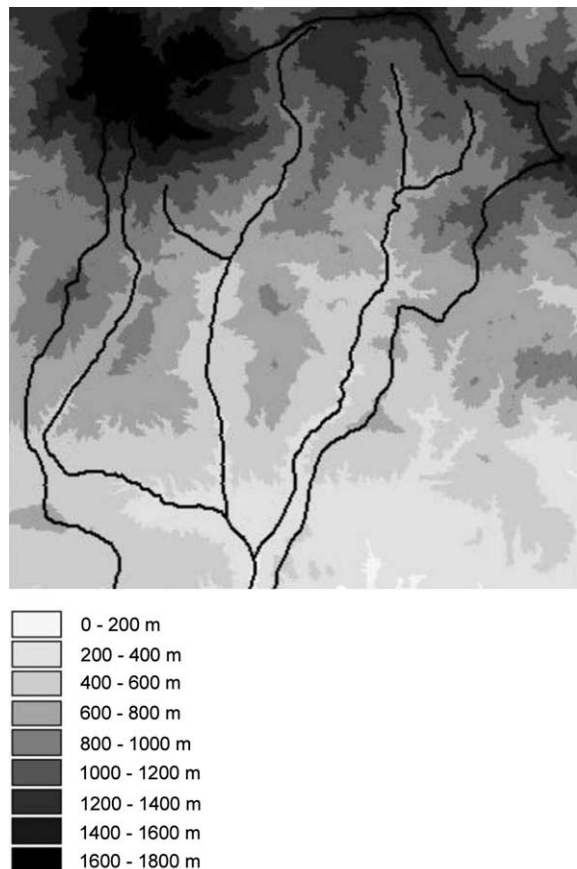


Fig. 2. Digital elevation model of the Kouris catchment.

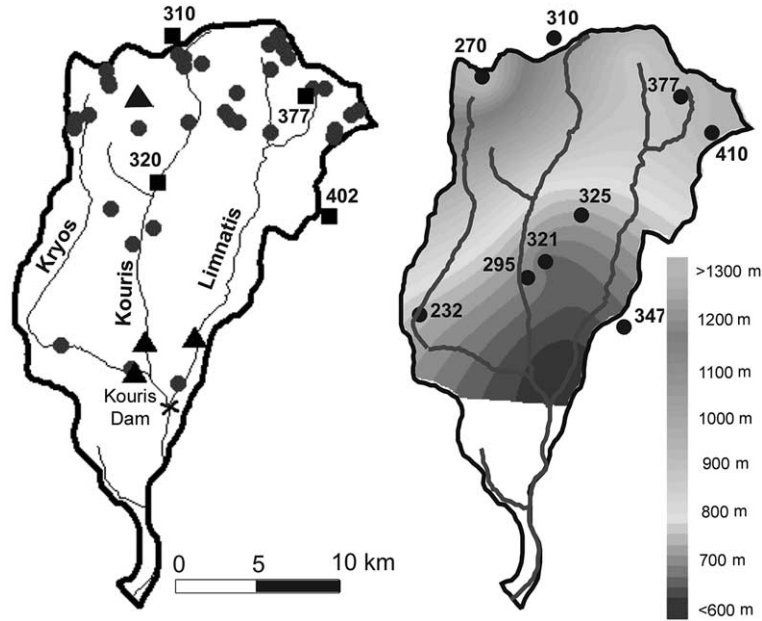


Fig. 3. Left: map of the Kouris catchment; circles—springs areas, squares—numbered climatological stations equipped for calculation of potential evapotranspiration; triangles—river gauges with recent measurements. Right: annual rainfall (1988–89) interpolated by linear kriging from nine meteorological stations (black circles with numbers).

potential groundwater contamination due to the asbestos mines in the north-west of the Kouris catchment. Within the LIFE project, water and rock samples from the igneous part of the Kouris catchment were analysed, and lineament analyses based on aerial photography were performed.

This paper presents an analysis of existing and new hydrogeological data, and combines them in a 2D regional groundwater flow model. The method of model calibration, which is based on hydrogram separation and spring discharge, provides a unique set

of hydrogeological parameters that will be required for more detailed future coupled surface/subsurface modelling. The focus of the present study is to estimate a range of the rates of recharge and analyse the likely impact of additional groundwater extraction. The results of the modelling are compared with estimates of the long-term average recharge derived independently using the chloride method. Finally, the sensitivity of the regional water balance to the different model inputs is evaluated, thereby pointing the way for future work.

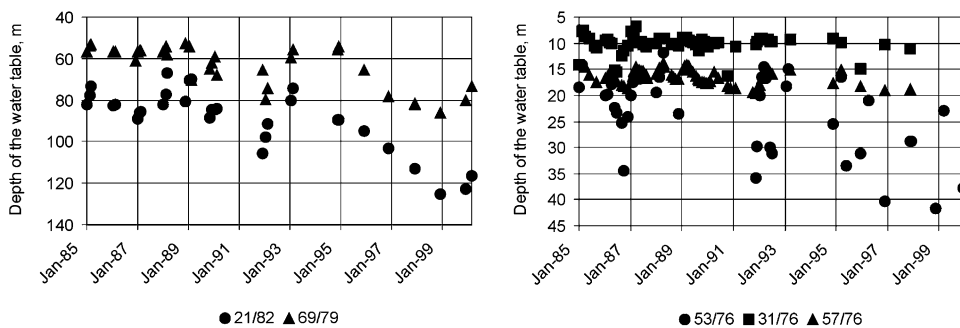


Fig. 4. Progressive increase in the depth of the ground water table in the extraction boreholes with serial numbers 53/76, 31/76, 57/76, 21/82 and 69/79 during non-pumping seasons (October to March).

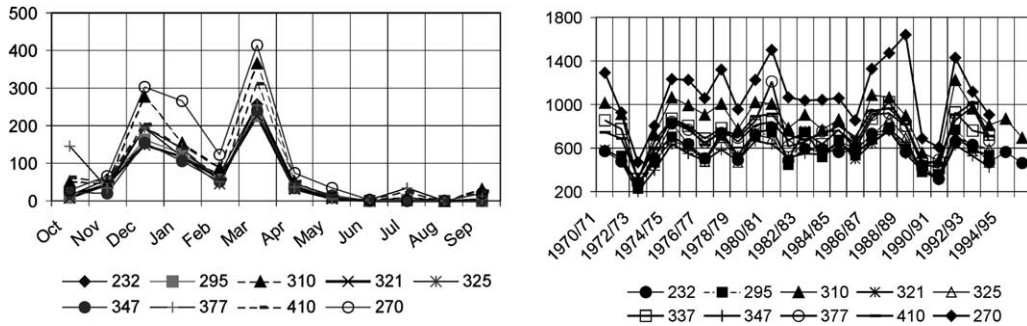


Fig. 5. Monthly (left) and annual (right) rainfall in mm at nine meteorological stations; numbers of meteorological stations are presented in the legend.

2. Data analysis

2.1. Precipitation

The long-term average annual precipitation for the Kouris catchment is 700 mm with 80% of it falling from November to March. Daily rainfall has been recorded at 18 meteorological stations since 1917 (Fig. 3); continuous daily records from splayed base rain gauges have been available at nine stations for the last thirty to forty years.

Annual rainfall correlates well with surface elevation (average correlation coefficient for 1970–1994 is 0.93), and is highly variable over the years (Fig. 5). No obvious trends can be identified during the period from 1970 to 1994. The maximum multi-year differences are found at high altitudes and can reach 900 mm (station N 270, hydrological years 1988/89 and 1989/90). Some dry periods (for example in 1972/73 and 1990/91) are noticeable at all stations (Fig. 5). Daily precipitation is highly variable in time

and space and cannot be described using simple correlation analysis.

2.2. Evapotranspiration

Cyprus has a typical Mediterranean climate with mild winters, long, hot, and dry summers, and short autumn and spring seasons. Climatic data (temperature, pan evaporation, humidity, wind velocity, etc.) have been recorded at four meteorological stations since 1984 by the Meteorological Department of Cyprus (Fig. 3). Daily potential evapotranspiration rates were calculated using a version of Penman’s equation with the net radiation term estimated from sunshine hours, using the software INSTAT (Stern et al., 1991, p. 49–51). The calculated mean annual potential evapotranspiration rate for the Kouris catchment for 1986–96 varies from 1060 to 1360 mm for the stations at different surface elevations. Within an annual cycle, the monthly potential evapotranspiration rate changes from less

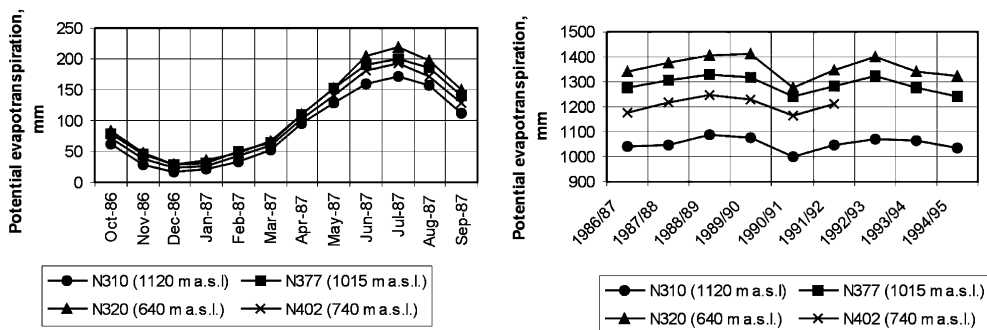


Fig. 6. Calculated monthly (left) and annual (right) potential evapotranspiration (Penman equation); numbers of meteorological stations are presented in the legends.

than 50 mm to more than 200 mm (Fig. 6). It is phase-shifted by half a year relative to monthly precipitation. Annual values stay nearly constant (with less than 10% variability) over the period of observations (Fig. 6).

2.3. Surface flow

The Kouris catchment is drained by three rivers: Kouris, Kryos and Limnatis (Fig. 3). Daily streamflow data is available from four gauging stations, although data collection at each began in different years. Three of them are located in the lower part of the three rivers and close to the Kouris Dam (Fig. 3). All the stations are equipped with permanently installed water level recorders and portable current meters that allow the measurement of flow velocities at different levels of water flowing through the station. The accuracy of the flow measurements is 5–10%, and is affected by the infrequency of flows, the steep gradient of riverbeds, and the movement of bed loads during floods.

Flow in the Kouris and Limnatis rivers persist throughout the year, consisting of spring water during the dry season, while the river Kryos is normally dry in summer. Daily streamflow reacts rapidly to rainfall—the peak of runoff occurs downstream only several hours after rainfall. The annual streamflow depends exponentially on the amount of precipitation (Fig. 7).

2.4. Geological setting

Cyprus and its immediate surroundings are segments of oceanic crust and mantle that are separated

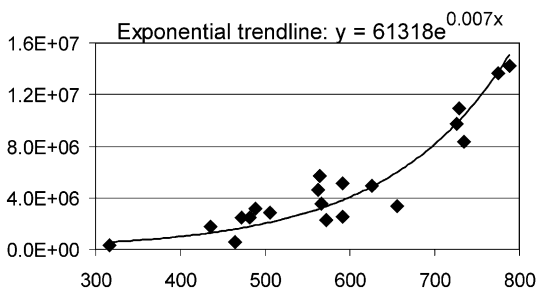


Fig. 7. Annual streamflow in the river Kryos as a function of annual weighted depth area precipitation across the Kryos subcatchment; the diamonds show values for the period of 1976–1996; the solid line is a calculated trend.

from the edge of one of the two major plates by rift-faulting—that developed possibly during the late Cretaceous (Malpas et al., 1990). The ophiolitic complex of the Troodos mountains, which is widely accepted as one of the best exposed on Earth, occupies an area of nearly 3000 km² in the south-western part of the island (Fig. 1). The plutonic complex is exposed in a central uplifted core and consists of tectonised harzburgites, dunites and serpentinites, stratigraphically overlain by ultramafic gabbroic cumulates. Due to subsequent erosion, the original upward succession of plutonic rocks, sheeted dike complex and pillow lavas is arranged in an outward succession from centrally exposed plutonic rocks to the sheeted dike complex and peripheral pillow lavas.

The simplified geological map of the Kouris catchment (Fig. 8) shows the two main geological zones: the ophiolitic complex in the North and the overlying sedimentary complex in the South. The ophiolitic complex is characterised by strong lithologic heterogeneity and is composed of different units: the pillow lava, the sheeted dykes, the gabbros and the peridotites. Inside these units, the sheeted dyke complex is heterogeneous because it is composed of a series of dykes of different ages with different compositions. These rocks have been altered either by

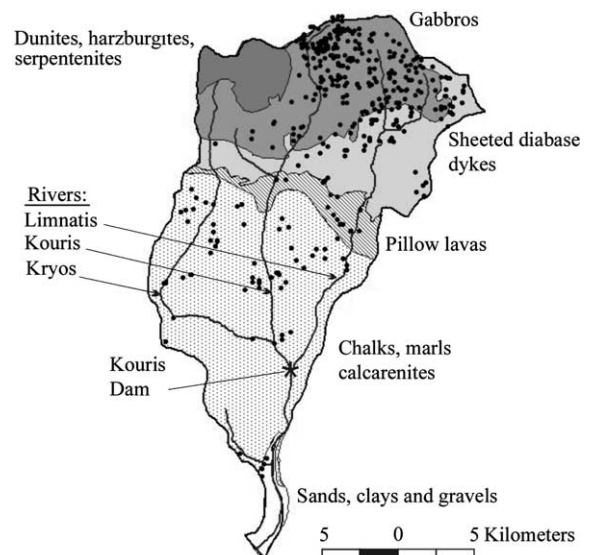


Fig. 8. Simplified geological map of the Kouris catchment; black circles show locations of boreholes drilled for irrigation purposes (some of them were unsuccessful).

hydrothermal circulation soon after their formation in an active rift or by recent weathering in surface. Finally, they are all fractured at different scales. The contact between ophiolites and sedimentary rocks has a tectonic origin and has been investigated by a number of studies (Gass et al., 1994), but the magnitude and the angle of the displacement within the area are still unknown.

2.5. Spring flow

Springs are mainly associated with plutonic and intrusive rocks (gabbro, sheeted dykes) in the upper part of the region. In total, 64 springs have been mapped within the catchment (Fig. 3) and 14 of the largest have been monitored monthly since 1986 by the Water Development Department. However, in the area with the most intensive groundwater extraction, spring discharge has not been measured. In addition, there are many small springs in the upper Limnatis subcatchment that are not mapped. The instantaneous discharge of one of the largest monitored springs (Mavromata) varies from 0.65 to 215 l/s. Considering only the monitored springs, we calculate minimum total spring discharges for the area ranging between 2 and 5 Mm³ per year, depending upon the year. The ratio between this amount and measured total stream-flow increases in dry years and can reach 20%.

2.6. Groundwater quality and occurrence

Generally, the catchment can be divided into two main aquifers: a sedimentary aquifer (chalks, marls, calcarenites) and an igneous rock aquifer (ophiolites) consisting of mantle, plutonic and intrusive sequences

The ophiolitic complex was identified as a major aquifer only comparatively recently when in the 70s drilling machines were imported into the island. The exploited groundwater resources lie in the fractured and altered rocks where the aquifer stays largely confined. Groundwater is generally of the CaMg–HCO₃ and Na–HCO₃ types with low to moderate salinities (300–600 mg/l), although cation and anion compositions vary considerably with local lithology (Afrodisis et al., 1986). The groundwater quality is generally adequate for domestic supplies and irrigation. The sedimentary aquifer in the south, which is composed mainly of chalks and marls, is less permeable and the groundwater has a higher salinity.

Table 1 shows a synthesis of drilling record information related to water occurrence in the different lithologies. In general, the boreholes are drilled to the second or third encountered fractured zone or up to a maximum depth of 250 m. The location of the boreholes is shown in Fig. 8. Information from a total of 166 boreholes is available. Of these, 64 boreholes were unsuccessful in finding sufficient water, and the rest found water in different

Table 1
Summary of drilling records in the Kouris catchment

Rock type	Boreholes with available records (since 1976)	Successful	Unsuccessful	Percentage successful boreholes (%)
Plutonic and intrusive sequence (gabbro and sheeted dykes)	83	77	6	93
Volcanic sequence (pillow lavas)	10	3 (basal group)	7 (6: upper and lower pillow lavas, 1: basal group)	30
Sedimentary rock (chalks, marls, calcarenites, alluvium)	73	22	51	30
Total within the area	166	102	64	61

quantities. Usually, water inflow during drilling occurs in the fractured zones in gabbros and sheeted diabase dykes, in the basal group of pillow lavas, in the river gravel near the surface, or in fractures in the sedimentary rocks. The few available records suggest a low probability of water occurrence in the pillow lavas.

In summary, the sediments can be considered to be an aquifer with little water available (30% drilling success in finding water), while drilling in the ophiolitic aquifer has a 93% success rate. These two aquifers are separated by Upper and Lower Pillow Lavas.

2.7. ^3H content in groundwater

Values of the tritium contents in groundwaters provided by [Jacovides \(1979\)](#) and [Verhagen et al. \(1991\)](#) allowed us to estimate residence times in the different aquifers. The calculation is based on the piston flow model ([Maloszewski and Zuber, 1982](#)), implemented in an EXCEL spreadsheet by Zoellmann (http://www.baug.ethz.ch/ihw/boxmodel_en.html), and uses the rainfall isotopic data for Cyprus provided by IAEA (<http://isohis.iaea.org>).

In the ophiolitic complex, the tritium content sampled in 14 springs in 1976–78 varied over a wide range (15–62 TU), which shows the complexity of the groundwater flow system in the fracture network. The calculated residence times are less than 5 years for 8 springs, 4–10 years for 4 springs and around 20 years for 2 springs. During the year, the tritium contents vary significantly. In March–April, the contents suggest that rainfall from the last rainy season contributes significantly to net discharge, while in autumn the vast majority of the discharging groundwaters tend to be several years older. The 20-year-old water seen at 2 springs appears only in the dry season. Boreholes tapping water in different depths show an even higher variability in tritium content than seen in springs. Boreholes which, are pumped heavily during dry seasons (typically for irrigation) sometimes eventually can even yield water that is older than 50 years, indicating extraction from old reservoirs. Such water cannot be considered renewable in the short term.

In the sedimentary complex, there is only one spring that has been sampled for tritium within

the alluvium in the Kouris catchment. The data indicate that the spring discharges recent water from the last flood. [Verhagen et al. \(1991\)](#) report analysis of groundwater from 28 boreholes that take water from the sedimentary complex to the west of Larnaka (approximately 30 km to the east of the Kouris catchment). Our calculations for 26 of these boreholes indicate residence times of about 25 years (1–6 TU in 1981–86), which is relatively long. This could reflect both low recharge rates and low flow rates coming from the ophiolites.

2.8. Aquifer properties

Data from 76 variable rate pumping tests are available. The drawdowns were recorded only in the pumping boreholes (i.e. not in observation wells). The duration of the pumping was usually 2–3 days, and the subsequent recovery was monitored. Some tests were repeated in different seasons and years. In many cases, the pumping rate varied considerably during the tests, sometimes by a factor of 5–6. Often, the water level in the borehole coincided with the level of the pump itself (which made interpretation more complex). All pumping test data were re-interpreted with PC software ([Sindalovski, 1999](#)) using the Theis solution superimposed in time for variable rates and recovery.

The resulting transmissivities are presented in [Table 2](#). Each interpretation is assigned a measure of quality between 0 and 4. The highest quality of 4 indicates that differences in values obtained from different tests or from pumping and recovery periods are all less than 20%. Similarly, 3 indicates differences between 20 and 200%. A quality factor of 2 indicates that only the recovery tests could be used, and 1 indicates that only the order of magnitude can be estimated. 0 indicates that the data cannot be interpreted. Overall, 15 values had grade 4, 24 values had grade 3, 15 values had grade 2, 12 values had grade 1, and 10 values had grade 0.

This data set is probably biased, as all boreholes were drilled in zones with potentially high transmissivity. Other concerns relate to the possible non-applicability of the Theis model because of well-bore effects, presence of single fractures, double porosity, non-integer flow dimensions, unconfined situations, spatial heterogeneities, etc.

Table 2

Results of pumping test interpretation. Coordinates are in UTM Grid 32, T = Transmissivity in m^2/day , q indicates the quality of the data (see text for explanation). Bh N-serial number of a borehole

Bh N	North	East	T	q	Type of rock	Bh N	North	East	T	q	Type of rock
71/92	484986	3851071	250	1	Alluvium/sediments	65/76	502336	3862271	159	2	Gabbro
34/96	484910	3850941	32	3	Alluvium/sediments	67/76	499413	3862237	20	4	Gabbro
156/85	495210	3857640	50	3	Dykes/gabbro	70/97	499453	3865604	50	3	Gabbro
42/86	495468	3857706	10	4	Dykes	76/92	497425	3863899	14	3	Gabbro
128/87	492097	3861336	153	2	Dykes/gabbro	81/81	485931	3861445	30	3	Gabbro
285/89	497520	3861525	7	1	Dykes/gabbro	82/99	503686	3862731	530	2	Gabbro
46/92	486130	3859354	20	1	Dykes/gabbro	84/88	502687	3864286	5	3	Gabbro
64/76	502711	3861596	46	2	Dykes/gabbro	85/96	498215	3863693	30	3	Gabbro
66/76	500603	3862240	27	0	Dykes/gabbro	86/86	487164	3861273	54	2	Gabbro
69/79/80	498675	3862076	100	0	Dykes/gabbro	87/84	492253	3861473	298	1	Gabbro
68/99	503406	3861816	4	4	Dykes/gabbro	94/96	502681	3862430	44	3	Gabbro
101/82	491870	3859785	25	3	Gabbro	95/87	500453	3866041	34	0	Gabbro
104/88	498703	3862897	7	0	Gabbro	A/T	495123	3863462	3	0	Gabbro
105/76	503661	3862663	70	2	Gabbro	v11/95	498145	3864780	56	3	Gabbro
118/88	502481	3857830	25	4	Gabbro	V2/94	494075	3859375	625	1	Gabbro
124/90	488164	3859812	10	4	Gabbro	w235/94	490727	3859699	200	1	Gabbro
133/90	498180	3867000	10	1	Gabbro	w235/95	495722	3863810	6	4	Gabbro
143/90	503284	3862413	5	3	Gabbro	w279/92	498275	3861504	5	4	Gabbro
158/87	499123	3863412	90	3	Gabbro	w288/91	494069	3865731	4	1	Gabbro
274/89	498155	3864600	160	0	Gabbro	w309/91	502986	3863054	350	1	Gabbro
30/74	486886	3860430	215	0	Gabbro	w35/93	502711	3864275	56	1	Gabbro
32/76	496618	3862619	3	2	Gabbro	w459/92	493694	3866581	9	4	Gabbro
32/96	494580	3863212	7	3	Gabbro	w471/90	497365	3863863	92	4	Gabbro
33/97	494095	3862994	83	3	Gabbro	w519/90	494379	3866436	4	4	Gabbro
40/96	493885	3868220	8	4	Gabbro	w54/74	496137	3867647	19	2	Gabbro
41/95	490590	3860800	25	3	Gabbro	w791/96	501313	3865028	4	3	Gabbro
46/97	494530	3863752	77	4	Gabbro	w82/92	493725	3863209	6	2	Gabbro
53/76	497588	3860394	703	2	Gabbro	19/76	493596	3866740	31	2	Gabbro/serpentinite
53/77	495973	3856571	9	3	Gabbro	31/76	493760	3864348	68	1	Gabbro/serpentinite
55/96	499475	3864667	11	3	Gabbro	36/96	490468	3860289	20	3	Gabbro/serpentinite
56/97	495677	3867864	4	4	Gabbro	15/94	487904	3853856	6	2	Sediments
57/76	498485	3864190	2	2	Gabbro	150/84	491745	3852393	23	2	Sediments
58/93	498350	3862635	40	4	Gabbro	22/94	490974	3851985	8	3	Sediments
58/96	501018	3864592	7	3	Gabbro	24/83	489590	3856002	2	0	Sediments
61/97	500718	3862327	9	4	Gabbro	31/95	492995	3847902	16	3	Sediments
62/76	498240	3866501	10	1	Gabbro	32/94	486990	3856550	5	3	Sediments
63/76	500943	3864350	100	0	Gabbro	73/84	491500	3839810	15	0	Sediments
63/93	499790	3862630	36	3	Gabbro	89/77	487667	3856140	11	2	Sediments

For the gabbros and sheeted dykes, taking only the 40 values graded '2' to '4', the distribution of transmissivity values is asymmetrical, with a high number of small values and only a few high values. It is approximately, but not perfectly, log-normal. The geometrical mean is $20 \text{ m}^2/\text{day}$ with minimum and maximum values of 2 and $703 \text{ m}^2/\text{day}$. The variance of the decimal logarithm of the transmissivity is 0.36. The spatial distribution of these transmissivities as described by their variogram does not show any clear

spatial structure. Nor do we observe a correlation between transmissivity and the lineament locations provided by [Charalambides et al. \(1998\)](#). Analysis of the geological logs from the boreholes shows that higher transmissivity values tend to be associated with fractured zones located at depths of several tens of metres and having widths, in certain cases, from 20 to more than 100 m. For the harzburgites, serpentinites, and pillow lavas, no pumping tests data are available within the catchment.

For the sediments, only six transmissivity values are suitable for interpretation (quality level 2 and 3). These vary from 2 to 23 m²/day with a geometrical mean of 9 m²/day. For the river bed alluvium, only two tests were conducted. These show high transmissivity values but with different quality: 32 m²/day (quality level 3) to 250 m²/day (quality level 1).

The thicknesses of the main aquifers is not known directly but can be inferred from geological observations, and by analogy with other mountainous groundwater flow systems in fractured rocks. The total thickness of the sheeted dykes is around 500 m and the thickness of the gabbros is up to kilometres (Gass et al., 1994). However, the hydraulic conductivity due to fracturing decreases with depth (van Everdingen, 1995). In the Alps, fractured crystalline rocks can be conductive even at depths exceeding a kilometre (Ofterdinger et al., 2002). Therefore, we envision the ophiolitic system to be a very thick body with a rather high degree of fracturing for the first 100–200 m and a progressive decrease of conductivity up to a depth of several kilometres. We can then expect very deep groundwater flow systems interacting with faster shallow systems. The pillow lavas formation has a thickness varying between 50 and 200 m. The thickness of the sediments varies between a few tens of metres in the north to more than 600 m in the vicinity of Lofou village, 9 km north-west of the Kouris Dam (Gass et al., 1994).

2.9. Piezometric surface

Measurements of the groundwater table were conducted by the Water Development Department of Cyprus and the Engineering Geology unit of Swiss Federal Institute of Technology as follows: (a) monthly in 17 boreholes since 1984, (b) continuously in 1 borehole since July 1992 and in 4 boreholes since spring 2000; (c) during one non-pumping period in 64 boreholes in March 2000.

The piezometric surface (Fig. 9) was constructed for March 2000 using the interpolated field observations of depths to the water table, a Digital Elevation Model with spatial resolution of 25 × 25 m (Hall, 1998), and a survey of the springs. Fig. 9 shows the piezometric surface of the catchment which follows the topography (Fig. 2) in a considerably smoothed manner.

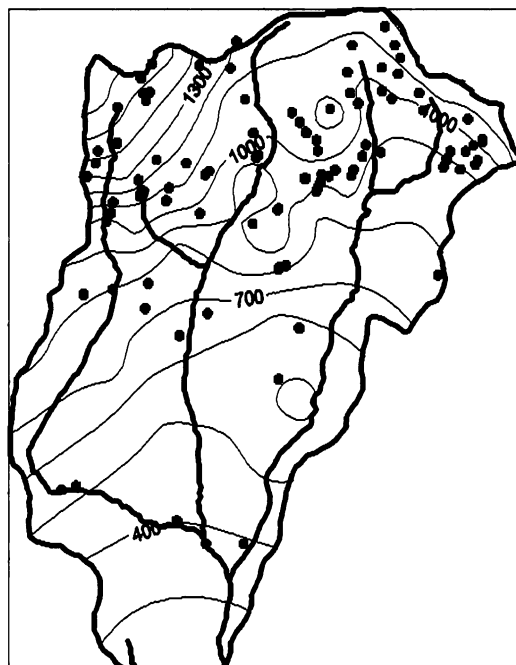


Fig. 9. Piezometric map constructed from interpolated piezometric heads for March 2000.

Variations in piezometric heads over many years range between several metres and 100 m. Annual variations normally do not exceed 30 m, although higher values can occur probably because of pumping (e.g. in borehole 109/77, where piezometric head variations of 60 m were measured in 1993). The lowest piezometric heads occur in September–October, while the highest occur in February–March.

2.10. Surface/ground water relation

Daily streamflow measurements in the lower part of the three rivers were used for hydrogram separation. We applied both the fixed-interval and the sliding-interval methods (Pettyjohn and Henning, 1979; Sloto and Crouse, 1996). The duration of surface runoff was estimated from the empirical relation (Linsley et al., 1982):

$$N = 0.83 A^{0.2},$$

where N is the number of days after which surface runoff ceases, and A is the drainage area in km².

Table 3
Separated hydrographs for the Kouris catchment. Rates are in Mm^3 per year

	Kryos		Kouris		Limnatis		Total	
	1988/89	1989/90	1988/89	1989/90	1988/89	1989/90	1988/89	1989/90
Streamflow	5.5	1.3	18.1	9.1	20.3	8.4	43.9	18.8
Baseflow from fixed-interval method (% of streamflow)	4 (73)	0.79 (61)	12.9 (71)	6.9 (76)	13.0 (64)	5.6 (67)	29.9 (68)	13.3 (71)
Baseflow from sliding-interval method (% of streamflow)	3.9 (71)	0.77 (59)	12.5 (69)	6.8 (75)	12.3 (61)	5.61 (67)	28.7 (65)	13.2 (70)

Drainage areas of 120 km^2 (Limnatis), 100 km^2 (Kouris) and 70 km^2 (Kryos) were used. The results of hydrogram separation for the years 1988/89 and 1989/1990, presented in Table 3, indicate that baseflow represents 60–75% of total streamflow.

2.11. Evaluation of recharge rate by the chloride method

We measured the chloride content in rainfall for the period September 2000–November 2001 at seven locations. Precipitation samples were combined either monthly or by rainfall events. The data of 29 rainfall samples indicated a homogeneous spatial and temporal distribution of chloride content, with an average value of 3.8 mg/l .

The direct recharge, R [m^3/year], was determined from the following chloride mass balance equation,

$$R = \frac{P \times C_p - S \times C_s}{C_r} \quad (1)$$

Here P [m^3/year] and S [m^3/year] represent, respectively, the long term averaged precipitation and surface run-off rates, while C_p , C_s , and C_r [mg/l] represent the chloride concentrations in precipitation, surface run-off and recharge. It is assumed that the amounts of chloride leaving the system via evaporation and entering the system via rock dissolution are negligible.

Hydrogram separations by the fixed-interval and the sliding-interval methods (Pettyjohn and Henning, 1979; Sloto and Crouse, 1996) show that the surface

runoff, S , is 30% of streamflow on average for the years 1986–1996. In addition, for this period the average annual ratio of rainfall versus streamflow is 0.16. Consequently we have $S = 0.16 \times 0.3 \times P = 0.05P$. The chloride concentration in surface run-off is generally close to the concentration in precipitation ($C_s = C_p$); however, this assumption leads to slight over-estimation of recharge for first rains after dry seasons when the surface run-off contains dissolved solids. Using these results in Eq. (1), together with the assumption that the concentration in recharge is close to the concentration in groundwater, C_g [mg/l], gives:

$$\frac{R}{P} = 0.95 \frac{C_p}{C_g} \quad (2)$$

We selected 70 sampling locations in the ophiolitic complex and four locations in the sedimentary complex chosen so that the samples were far enough from the rivers to avoid mixing with surface water from floods. The measured concentrations were between 7 and 26 mg/l in the ophiolitic complex, and between 23 and 30 mg/l in the sedimentary complex. This leads to local recharge rates ranging between 14 and 52% in the ophiolites and between 12 and 16% in the sediments. An estimate of the average chloride concentration for the catchment is calculated by weighing the averaged values within each of the lithologies by the relative surface areas they occupy in the catchment. The results indicate $C_g = 21 \text{ mg/l}$ and an average recharge rate of 17%.

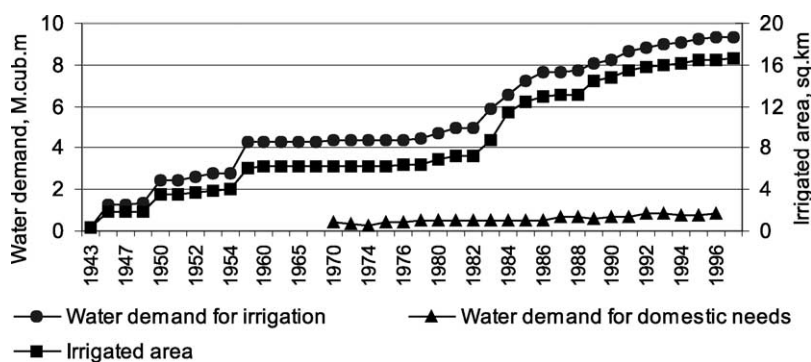


Fig. 10. Water demand for the irrigation and domestic needs of the Kouris catchment.

2.12. Land use and water extraction

Water extracted upstream of the Kouris Dam is used both for irrigation (mostly) and for domestic needs. The irrigated surface is approximately 17 km² and is covered by deciduous trees, vineyards and to a lesser extent by seasonal crops. The exact amount of present groundwater extraction is unknown. However, water demand upstream of the dam, estimated by the Water Development Department based on types of crops, irrigation area and number of inhabitants, was more than 10 Mm³ per year in 2000 (Fig. 10).

Water demand is satisfied either by stream water, diverted from rivers or collected at the local dams, or by groundwater, pumped from boreholes or diverted from springs. Stream water is normally collected during the whole year and applied in summer for irrigation, while groundwater is extracted during summer and autumn. A rough estimate of actual ground and surface water extraction suggests that the most intensive pumping occurs in the upper parts of Limnatis and Kouris subcatchments.

3. Groundwater flow modelling

Despite all the evidence that the aquifer is fractured, we modelled it as a continuous porous medium. This approach is reasonably correct for a regional study of water balance (see NRC (National Research Council), 1996 for a review). All the heterogeneities due to the presence of a dense network of fractures and dykes which have a scale of a few

metres in width and between tens and hundreds metres in length are averaged in an equivalent isotropic transmissivity which is constant at the scale of the geological formation (several kilometres). In practice, the groundwater flow was simulated in steady-state with a finite-difference technique using the code MODFLOW (Harbaugh and McDonald, 1996) with the PMWIN interface (Chiang and Kinzelbach, 2001). The hydrological year 1988/1989 (01.10.88–30.09.89) was chosen because the rainfall in that year was close to the long-term average. Another reason is that human impact on groundwater was still small at that time, while it seems have been very high since 1995.

3.1. Model configuration

The boundary of the surface catchment was derived from the Digital Elevation Model (Hall, 1998) and assumed, in the first step, to coincide with aquifer boundaries. In the second step this assumption was tested. The catchment was modelled as a confined aquifer with recharge imposed on the top. The area was discretized as one layer with a regular grid (250 m × 250 m, 142 rows by 86 columns). Fig. 11 shows the grid and the location of the different boundary conditions. The boundaries are taken as impervious except along the Mediterranean coast where a fixed-head boundary condition, $h = 0$ m, was imposed. The rivers Kryos, Kouris and Limnatis were incorporated into the model using the River Package of MODFLOW. The elevations of the river bottom were obtained from interpolation of

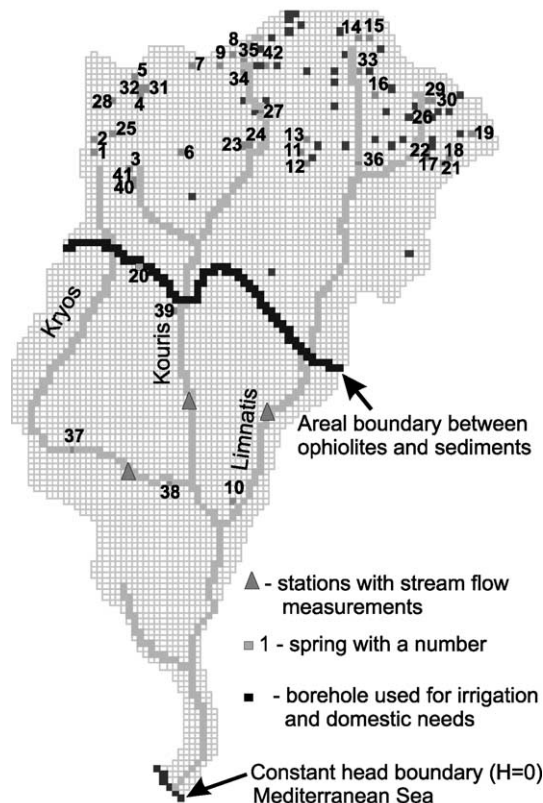


Fig. 11. Map showing the location of boundaries for the modelling of the Kouris catchment.

the Digital Elevation Model; the water levels in the rivers were specified to be 0.5 m higher than the surface; the hydraulic conductances of the riverbed was determined by model calibration. Forty-two spring areas were incorporated into the model with the Drain Package of MODFLOW. The elevations of the drains were derived from the Digital Elevation Model and modified during model calibration. The drain hydraulic conductances were determined during the calibration procedure. Forty zones of groundwater pumping were imposed with constant pumping rates equal to the estimated annual extraction amounts for 1988/89.

3.2. Recharge

Four zones of recharge were defined (Fig. 12(a)) based on the geology and on the assumption that

recharge is controlled by precipitation and evapotranspiration, which have correspondingly positive and negative correlations with surface elevation.

The total regional rainfall for the modelled year was calculated with the ISATIS package (<http://www.geovariations.fr>). The annual rainfall from nine meteorological stations was interpolated by linear kriging inside the catchment boundaries on a 50 m by 50 m grid (Fig. 3). The total rainfall was the sum of the raster values multiplied by the area of the grid cell and was 241 Mm³.

Two variants of recharge were modelled. Variant 1 was the conservative one for water management (minimum recharge) and assumed that all recharged water left the area via baseflow upstream of the Kouris dam and springs discharged into the rivers. No water was presumed to leave the model area via underground flow, recharge spent for increasing groundwater storage was neglected, and spring flow was included in river baseflow. Hence, total recharge for the four zones was adjusted to 30 Mm³ to agree with the results of hydrograph separation for the three rivers (Table 3). This amount equalled to 12.5% of total annual rainfall, and was in agreement with estimates from other studies that suggest that recharge in the range of 10–15% of the total rainfall for some areas on the coast (Jacovides, 1982; Schmidt et al., 1988). Higher values probably apply to the ophiolitic complex, as it is at a higher surface elevation, and this was suggested by the chloride balance calculation. The total recharge was distributed over the four zones (Fig. 12(a)) according to the assumption that recharge increases with altitude. The largest differences in recharge rates were expected between Zones C and D and were caused both by differences in altitude and the relatively small infiltration capacity of sedimentary rock compared to ophiolites.

Variant 2 was the maximum recharge scenario. It was developed to test the sensitivity of the model to the recharge rate and to check what could be the maximum reasonable recharge rate. According to the general water balance for Cyprus (Omorphos et al., 1996), 80% of rainfall is evaporated, while the remaining 20% constitutes the water resources that are available for recharge and runoff. In Variant 2, 20% of the annual rainfall (i.e. about 48 Mm³ for 1988/1989) was used as recharge.

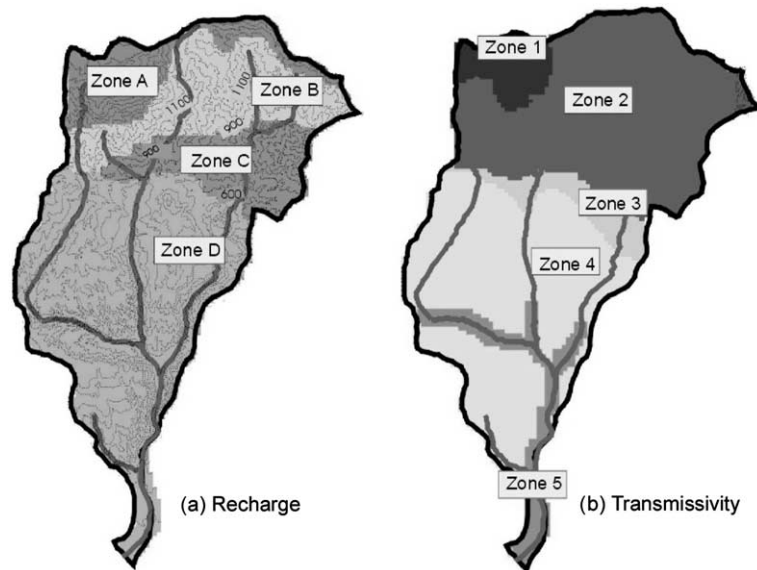


Fig. 12. Left: recharge zonation depending on the surface elevation. Right: transmissivity zonation (Zone 1—harzburgites, serpentinites; Zone 2—gabbro, sheeted dykes; Zone 3—pillow lavas; Zone 4—sediments (chalks, marls, calcarenites); Zone 5—alluvium).

3.3. Transmissivity

Five zones of transmissivity were distinguished according to regional geology and pumping test results (Fig. 12(b)). These were: Zone 1—mantle rocks (harzburgites, serpentinites, dunites); Zone 2—plutonic and intrusive rocks (sheeted dykes and gabbros); Zone 3—volcanogenic rocks (pillow lavas); Zone 4—sedimentary rocks (chalks, marls, calcarenites); Zone 5—sedimentary rocks (alluvium in the river beds).

For zones 2 and 5, the initial values for the regional transmissivities were estimated by multiplying the percentage of successful boreholes drilled within a lithology by the geometrical mean of the transmissivities obtained from pumping test interpretation. The resulting values were $T = 0.93 \times 20 = 19 \text{ m}^2/\text{day}$ for the gabbros and sheeted dykes (Zone 2), and $T = 3 \text{ m}^2/\text{day}$ for the sediments (Zone 4). The transmissivity of Zone 1 (mantle rock) must be lower than that of Zone 2 because the rocks are more massive, while the transmissivity of the alluvium (Zone 5) was expected to be higher than that of the surroundings (Zone 4). Thus, $9 \text{ m}^2/\text{day}$ and $6 \text{ m}^2/\text{day}$ were used as initial values for zones 1 and 5. In the case of Zone 3 (pillow lavas), 7 out of 10

boreholes did not reach the water table, and one pumping test conducted outside the Kouris catchment gave a moderate transmissivity value ($10 \text{ m}^2/\text{day}$). Thus, an initial value of $1 \text{ m}^2/\text{day}$ was used for Zone 3. Note that fractures are expected in pillow lavas and therefore the regional transmissivity could be higher in this lithology.

3.4. Model calibration

The model was calibrated manually by trial and error using the following procedure. First, the transmissivity of Zone 1 was adjusted such that the variance of the difference between measured and calculated heads was a minimum. Then, the same was done successively for the transmissivities of zones 2, 3, 4 and 5. When this was achieved, the values of the recharge rates were adjusted within the different zones to again minimise the variance of the head differences, subject to the constraints that the total recharge remained constant and that the zones at higher altitudes had higher recharge rates. The next step was to adjust the values of the river bed conductances and drain altitudes so as to match the discharge rates in rivers and springs with their measured values. Finally, the variance of the head differences was

Table 4
Calibrated set of parameters for variant 1 and variant 2

Parameter	Value for variant 1	Value for variant 2
Transmissivity of zone 1	4.5 m ² /day	6 m ² /day
Transmissivity of zone 2	16 m ² /day	30 m ² /day
Transmissivity of zone 3	100 m ² /day	250 m ² /day
Transmissivity of zone 4	1 m ² /day	1.5 m ² /day
Transmissivity of zone 5	20 m ² /day	40 m ² /day
Recharge of zone A	248 mm/year	372 mm/year
Recharge of zone B	168 mm/year	292 mm/year
Recharge of zone C	146 mm/year	219 mm/year
Recharge of zone D	11 mm/year	16 mm/year
Hydraulic conductance of the riverbed (most of the rivers)	25 m ² /day	50 m ² /day
Hydraulic conductance of the riverbed (small parts upstream of Kryos and Kouris containing possibly only water from springs)	0.02, 0.2, 2 m ² /day	0.02, 0.2, 2 m ² /day

checked, and all the steps repeated in sequence until an acceptable variance was obtained. Three loops were required until the expected accuracy was achieved.

An important point was the criteria to decide when a reasonable fit was obtained. We arbitrarily considered the errors in heads below 100 m to be reasonable. Our arguments were first, that the topography is steep in the upper part of the catchment (local slopes between 15 and 30%, sometimes up to 40%). Thus, differences in surface elevations can reach 100 m within the distance of 250 m (the size of a model cell), which brings the uncertainty equal to 100 m in piezometric heads, calculated from depths of the water table and surface elevations. Second, for the model calibration we used piezometric data from different years and 100 m is considered to be the maximum of long-term variations of piezometric heads. Thus, attempting to increase model accuracy necessarily leads to a reduction in the quantity of data used in the calibration. Finally, 100 m represents only 6–7% of the difference between the lowest and highest piezometric heads of the area.

The resulting set of calibrated parameters is listed in Table 4. With the exception of those for the pillow lavas, transmissivity values were modified only slightly during the calibration procedure. The observed and simulated discharges agree to within 92%, and the corresponding scatter diagram of heads for Variant 1 is presented in Fig. 13. Table 5 lists estimated and simulated river and spring discharges

for Variant 1, and shows that there is satisfactory agreement between modelled river discharges upstream of the three river gauges and the baseflows obtained from hydrogram separation. When it was assumed that the springs were flowing to the rivers, the resulting simulated baseflow differed from the total observed baseflow by 4–8% (Table 5) depending on the method used for hydrogram separation.

The analysis of the spatial distribution of simulation errors indicates that no zones occur with systematically positive or negative errors. There are small simulation errors in the upper part of the Kryos subcatchment, while in the upper part of the Limnatis subcatchment high positive and negative errors often appear close to each other. This could be the result of

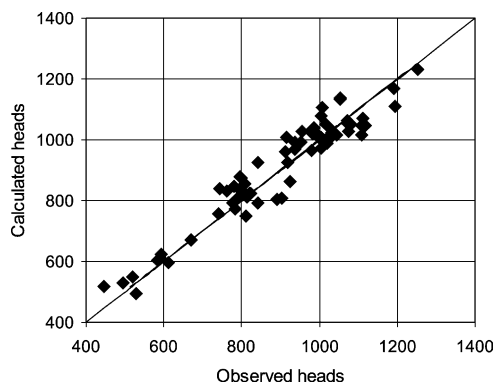


Fig. 13. Scatter diagram for observed and simulated heads in 71 boreholes, Variant 1; calculated variance is 2550 m².

Table 5

Estimated and simulated (variant 1) components of outflow upstream of the Kouris dam, in Mm³ per year

River subcatchment upstream of Kouris Dam	Baseflow from hydrograph separation for 1988/89		Modelled discharge		
	Fixed-interval method	Sliding-interval method	Rivers	Springs	Rivers and springs
Kryos	4.0	3.9	1.3	0.3	1.6
Kouris	12.9	12.5	9.1	1.8	10.9
Limnatis	13.0	12.3	12.8	1.3	14.1
Total discharge upstream the Kouris dam	29.9	28.7	23.2	3.4	26.6

either strong rock heterogeneity in the north-eastern part of the catchment, or it could indicate the depletion of a compartmentalised groundwater reservoir due to over pumping.

The uncertainties in spring locations, elevations and total discharges are large, and so, could be taken into account only approximately. Another problem in spring simulation occurred because hydraulic gradients controlling spring discharge are normally influenced by local parameters and hydrodynamic head distributions, which are neither resolved by the field information available nor by the model grid. In some springs, the actual discharge was unknown. In those cases, any computed discharge was counted as a satisfactory result. In the absence of other information, a large value of 10,000 m²/day was assigned to drain hydraulic conductance, and the elevation of drain was set to the value derived from the Digital Elevation Model. Usually the latter value had to be

reduced by up to 100 m to obtain reasonable discharge rates.

3.5. Model results

The resulting estimates of the total water balance of the Kouris catchment for 1988/1989 for variants 1 and 2 are presented in Table 6. The simulated and observed heads agree with the satisfactory accuracy of the estimate (Fig. 13). Fig. 14 shows the simulated piezometric map for variant 1. Water balance calculations for different regions show that the groundwater flow from the gabbros and sheeted dykes to the sediments through the pillow lavas is high: about 6–7 Mm³/year. Later, most of this water is discharged as river leakage into the upper part of the sediments and pillow lavas, and to a lesser extent, through springs in the sedimentary rocks. Groundwater outflow to the Mediterranean Sea is the smallest

Table 6

Water balance for the Kouris catchment, with all values in Mm³ per year for 1988/1989; variants 1 and 2

Inflow	Variant 1	Variant 2	Outflow	Simulated		Reference ^a
				Variant 1	Variant 2	
River leakage	0.8	1.7	Groundwater outflow into the Mediterranean Sea	0.1	0.3	NA ^b
Recharge	30.2	48.0	Springs discharge	4.2	4.9	>3.7
			Groundwater extraction	1.7	1.7	1.8
			Discharge in the river Kryos	1.6	1.3	3.9
			Discharge in the river Kouris	10.9	15.6	12.7
			Discharge in the river Limnatis	13.1	22.8	12.7
			Sub-total all rivers	25.0	42.7	29.3
Total	31.0	49.7	Total	31.0	49.6	>34.8

^a Reference from Table 3. Note that for the variant with big recharge 12 simulated springs from 42 turned out to be dry.

^b NA = Not available

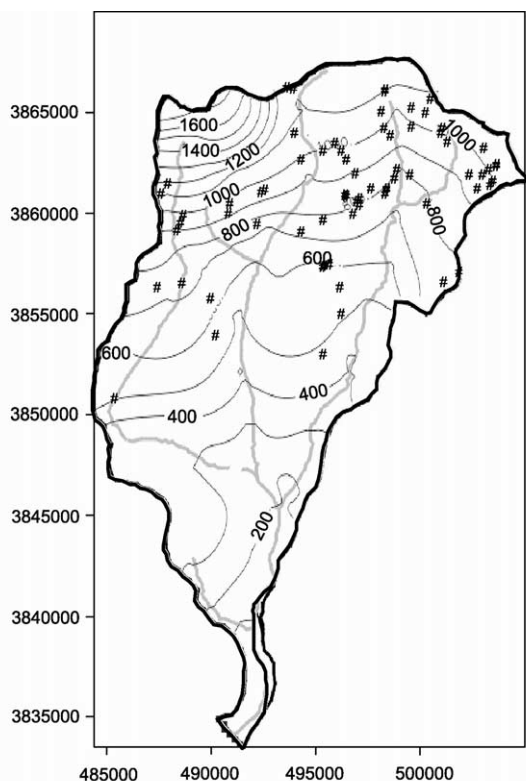


Fig. 14. Map showing contours of piezometric heads for the simulation of Variant 1.

discharge component. Variant 2 also gives satisfactory simulated heads, with the exception of four boreholes where the errors are slightly larger than 100 m. Thus, a calibration based only on heads would not be unique since two calibrated sets of parameters could result in completely different water management scenarios. However, Variant 2 can be discounted for other reasons: the predicted total river leakage is too high (Table 6), the ratios between leakage fluxes in the three rivers are incorrect (Table 6), the transmissivity of 30 m²/day of Zone 2 is unreasonably high, and spring elevations must be lowered more than is acceptable in order to obtain the correct discharges. A third variant with recharge equal to 16% of rainfall gives a reasonable calibrated transmissivity for Zone 2 of 20 m²/day and an acceptable water balance. Thus, within the assumptions of this model, the annual actual recharge for 1988/89 is estimated to be between 12 and 16% of total rainfall.

The location of the groundwater catchment boundaries is uncertain, since they might not coincide with their surface expressions. This uncertainty is highest in the sediments in the south where the surface catchment becomes very narrow. In order to check the model sensitivity to this parameter, the model boundaries were extended significantly in the sediments to construct Variant 4 (Fig. 15). All other parameters were kept the same as in Variant 1. The resulting water balance, presented in Table 7, shows that the groundwater flow to the sea remains less than 2% of the total outflow and that the other components of the water balance are not changed considerably.

The impact of groundwater extraction in 1988/89, predicted by model Variant 1, is very limited. The average water levels are different from those of the model run without pumping by only 10 m. A further modelling variant (Variant 5) assumes that all extraction rates were higher by a factor 5 (i.e. 8.77 Mm³/year in total), which approaches the present level of water demand. Again, all other parameter values are kept identical to those in Variant 1. The results of this simulation

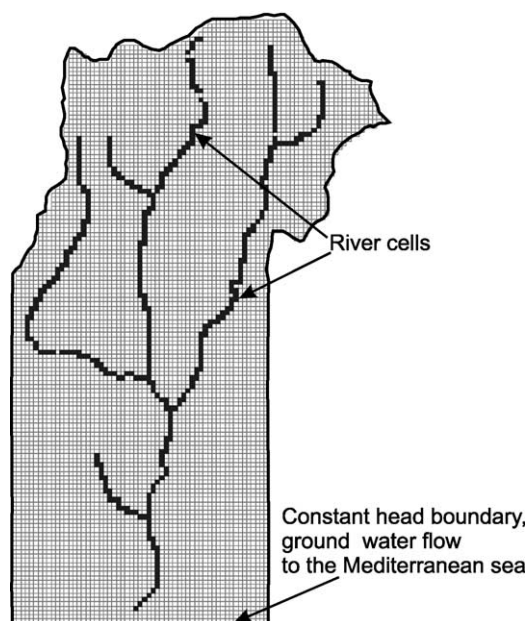


Fig. 15. Map showing the location of extended catchment boundaries for the sensitivity analysis.

Table 7

Water balance of the Kouris catchment with extended boundaries (all values in Mm^3 per year); variants 4 and 5

Inflow	Variant 4	Variant 5	Outflow	Variant 4	Variant 5
River leakage	0.7	0.8	Groundwater outflow into the mediterranean sea	0.6	0.1
Recharge	32.0	30.2	Spring discharge	4.4	2.7
			Discharge to the rivers	26.0	19.5
			Groundwater extraction	1.7	8.8
Total	32.7	31.0	Total	32.7	31.1

are shown in Fig. 16 and Table 7. Increasing groundwater extraction reduces mainly the baseflow in the upstream parts of the Kouris and Limnatis subcatchments from 25 to $18 \text{ Mm}^3/\text{year}$. This would represent a $7 \text{ Mm}^3/\text{year}$ deficit of inflow for the Kouris dam. Of the 42 springs, the 14 closest to the pumping boreholes (33%) dry up.

The total spring discharge is reduced by 36% compared to Variant 1. Additional drawdown occurs only in the upstream of the Kouris and Limnatis subcatchments over an area of about 50 km^2 . In this area, drawdowns increased by 30 m on average and reached 180 m around pumping boreholes.

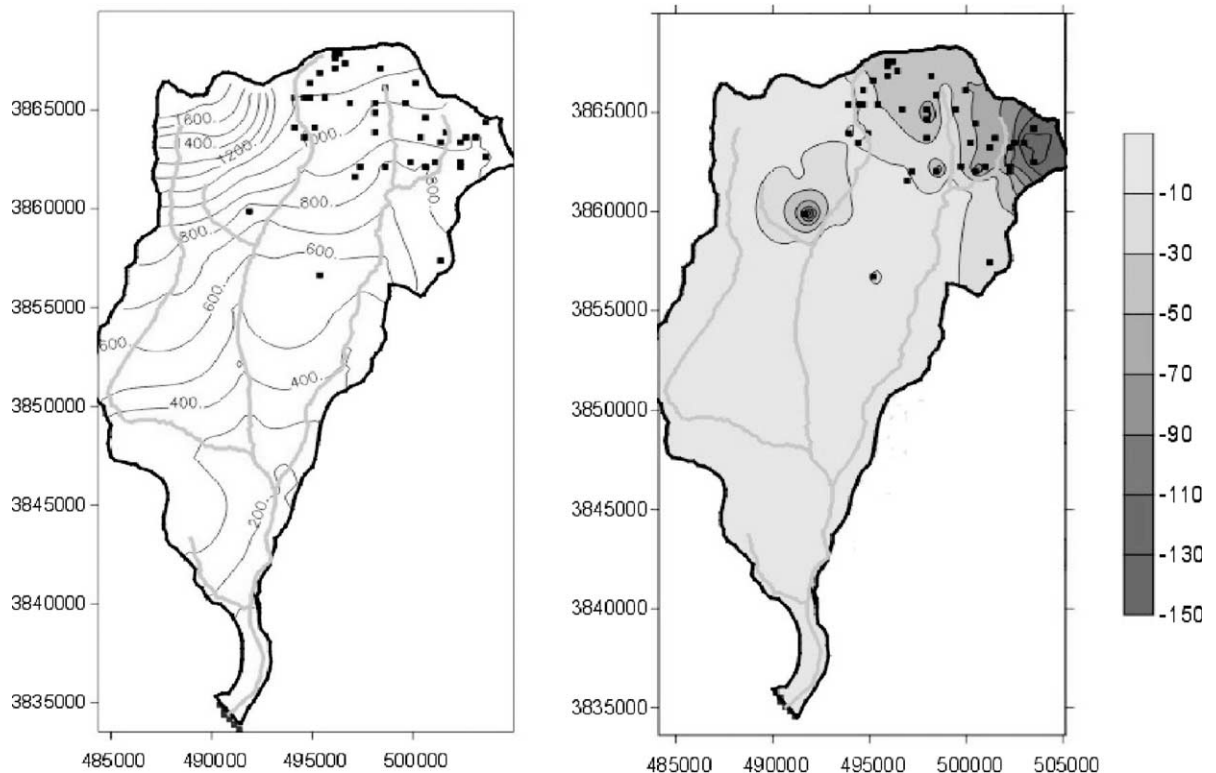


Fig. 16. Results of simulation with 8.77 Mm^3 annual groundwater pumping: Left—piezometric map; Right—differences to the basic variant (colour scale is in metres).

4. Discussion

Under the current state of knowledge of groundwater in the Kouris catchment, our model yields estimates for the recharge rate of between 12 and 16% of annual rainfall for 1988/89. This is in agreement with the chloride mass balance data and is relatively insensitive to the geometry of the catchment boundaries in the sediments.

The model can be used to forecast possible impacts of increased exploitation. This was demonstrated in Variant 5 and could be extended to even higher exploitation rates. However, the model is not able to evaluate the time scale on which the baseflow will react to such increased exploitation. Such an investigation would require a transient model to be constructed. In addition, the model is not able to forecast the effect of potential variations in precipitation and temperature due to climatic change, as the recharge is not calculated from these meteorological data but calibrated. Furthermore, because of its steady-state assumptions, the model cannot be used to forecast some more subtle effects such as the shift of precipitation from one season to another, as observed for example by [Kypris \(1995\)](#) in Cyprus. Overcoming these limitations requires a more sophisticated transient model that couples groundwater and surface flow, and allows precipitation, rather than recharge, to be input directly.

The constraints applied in the present model are the head data, the baseflow estimated from hydrogram separations, the transmissivities estimated from pumping tests, and the spring discharges. The accuracy of the model is therefore directly linked to the accuracy of these data. The results obtained show that the most important constraint is the baseflow. Uncertainty in its value arises from errors in streamflow measurements and errors due to the estimation methods. The estimation methods that can be used include: tracer methods ([Stichler et al., 1986](#)), field methods requiring boreholes in the alluvial aquifer or seepage meter installations ([Cruickshank et al., 1988](#); [Holko, 1995](#)), and methods using only streamflow observations ([Nathan and McMahon, 1990](#)). The curve-fitting techniques used for the Kouris catchment ([Sloto and Crouse, 1996](#)) belongs to the last group of methods. The most reliable

hydrogram separations can be obtained by a combination of several methods. Unfortunately, at present only streamflow observations are available in the catchment. Thus, baseflow was calculated using only one type of method. Nevertheless, curve-fitting (in our case fixed-interval and sliding interval methods) is widely accepted by hydrologists for hydrograph separation even in mountainous regions (e.g. [Lindsey et al., 1997](#); [Sinclair and Pitz, 1999](#)). Certainly, since the absolute value of the baseflow is the most important constraint, tracer methods should be applied in the future.

Improved estimates for spring locations and elevations would also be useful for constructing the piezometric head field. However, better measurements of spring discharge will not significantly improve total water balance calculations.

The calibrated transmissivity of the gabbro/sheeted dykes complex varies within a small range (16–20 m²/day) and coincides with the geometrical mean of all pumping test interpretation results. The modelled piezometric map is highly sensitive to the transmissivity of mantle rock, which according to the model calibration can vary over a very small range of 4.5–5.5 m²/day. These results are comparable, at least in terms of contrast between the hydraulic conductivities of different lithologies, with the pumping test estimates of [Dewandel et al. \(2002\)](#) for the ophiolite rocks of Oman.

A striking feature of the model is the groundwater flow that is predicted to occur from the gabbros and sheeted dykes to the sediments through the pillow lavas. Additional investigations should be conducted in order to check the validity of this calculation. This could be achieved by model calibration with additional streamflow measurements that would give a more detailed river leakage distribution, and could be tested with a comparative study of isotopic signatures of groundwater on both sides of the contact.

As we have already discussed, the accuracy of the head values is very limited in our model. This is not a problem for the regional water balance, but it would not be acceptable for a groundwater management model. If such a model was constructed, it would obviously have to be focused on the gabbros and sheeted dykes area in the upper Kouris and Limnatis subcatchments where groundwater extraction is the highest.

5. Conclusions

The Kouris catchment is a Mediterranean and partially (in the southern part) semi-arid area with scarce water resources and where water conflicts are increasing dramatically. The area has suffered a sustained long-term reduction of surface/ground water storage. The area is characterised by high heterogeneity of rock properties, major evapotranspiration losses during the dry season, and strong coupling of surface and ground water.

Groundwater flow modelling of the area for the year 1988/89 indicated that recharge was between 12 and 16% of the total annual rainfall, which amounted to 100–150 mm for that year. Specifying recharge rates of less than 12% led to insufficient water supply for the estimated baseflow, whereas recharge of 20% already produced unacceptable changes in the predicted ratio between flows of the three rivers of the catchment. The chloride method gives an estimated long-term average recharge equal to 17% of rainfall, which is in agreement with the model.

If the current water demands were solely satisfied by groundwater, very high drawdowns in some locations of the catchment would likely occur. It is also very probable that spring discharge would be severely reduced, perhaps by as much as a factor two, resulting in the drying up of many springs. Furthermore, the natural discharge of the aquifer into the rivers could drop from 25 to 18 Mm³ per year, thereby reducing significantly the annual inflow into the Kouris dam.

Whilst the results have serious implications for groundwater in Cyprus, they must be considered provisional owing to the many uncertainties in the model. To improve the accuracy of the simulation at the regional scale, additional streamflow measurements combined with isotopes investigations should be conducted and the flow through pillow lavas should be estimated. The development of a transient model could allow the transition time between the natural and the perturbed situation to be assessed. Finally, substantially improving forecasts for groundwater management requires that the area in the upstream of Kouris and Limnatis Rivers be further investigated.

Acknowledgements

The authors thank W. Kinzelbach, F. Leuenberger, C. Leduc, K. Evans and D. Porcelli for their comments and suggestions. We are also grateful to A. Moll, M. Steiner, U. Jorin and S. Oertli for essential contributions during their diploma studies. The work was financially supported by the European Commission: Research Project BBW 97.0621 and by the Swiss Federal Institute of Technology.

References

- Afrodisis, S., Avraamides, C., Fischbach, P., Hahn, J., Udluft, P., Wagner, W., 1986. Hydrogeological and hydrochemical studies in the Troodos region. Technical Report N6 in Cyprus—German Geological and Pedological Project No. 81.2224.4. Ministry of Agriculture and Natural Resources, Geological Survey Department, Nicosia, Cyprus, p. 101.
- Charalambides, A., Kyriacou, E., Constantinou, C., Baker, J., van Os, B., Gurnari, G., Shiathas, A., van Dijk, P., van der Meer, F., 1998. Mining Waste Management on Cyprus. Final report, LIFE project, ITC, Enschede.
- Chiang, W.-H., Kinzelbach, W., 2001. 3D Groundwater Modelling with PMWIN, Springer, Berlin, p. 346.
- Cruikshank, F.B., Francis, R.M., Jardine, D.E., 1988. A study of groundwater/surface water interaction in the Winter river, Prince Edward Island, using seepage meters and minipiezometers. In: Lin, C.L., (Ed.), Proceedings of International Groundwater Symposium on Hydrogeology of Cold and Temperate Climates and Hydrogeology of Mineralized Zones, International Association of Hydrogeologists, Canada, pp. 29–40.
- Dewandel, B., Lachassagne, P., Boudier, F., Ladouche, B., Pinault, J.L., Quatan, A., 2003. Hydrogeological Structure and Functioning of a Hard-rock Aquifer: The Oman Ophiolite, Submitted for publication.
- van Everdingen, D.A., 1995. Fracture characteristics of the sheeted dyke complex, Troodos ophiolite, Cyprus: implications for permeability of oceanic crust. *Journal of Geophysical Research* 100 (B10), 19957–19972.
- Gass, I.G., MacLeod, C.J., Murton, B.J., Panayiotou, A., Simonian, K.O., Xenophontos, C., 1994. The geology of the Southern Troodos transform fault zone. Memoir No. 9. Geological Survey Department, Ministry of Agriculture, Natural Resources and Environment, Nicosia, Cyprus, p. 218.
- Gillis, K.M., Sapp, K., 1997. Distribution of porosity in a section of upper oceanic crust exposed in the Troodos ophiolite. *Journal of Geophysical Research* 102 (B5), 10133–10149.
- Hall, J.K., 1998. Digital terrain model (DTM) of the Island of Cyprus. *CSI Current Research* 11, 45–50.
- Harbaugh, A.W., McDonald, M.G., 1996. User's documentation for Modflow-96, an update to the US Geological Survey modular

- finite-difference ground-water flow model. Open-File Report 96-485, US Geological Survey, p. 56.
- Holko, L., 1995. Application of stable environmental isotopes in hydrological research of a mountain catchment (in Slovak). PhD Thesis, Institute of Hydrology SAS, Bratislava, p. 100.
- Jacovides, J., 1979. Environmental isotope survey (Cyprus). Final report on IAEA, Research Contract No: 1039/RB, Technical Report. Ministry of Agriculture and Natural Resources, Department of Water Development, Nicosia, Cyprus, p. 82.
- Jacovides, J., 1982. Southern conveyor project, feasibility study: groundwater resources, vol. 3. Technical Report. Ministry of Agriculture and Natural Resources, Water Development Department, Nicosia, Cyprus, p. 77.
- Jacovides, J., 1997. Artificial groundwater recharge practice in Cyprus. In: Simmers, I., (Ed.), Recharge of Phreatic Aquifers in (Semi-) Arid Areas, International Association of Hydrogeologists Monograph 19, pp. 201–215.
- Kitching, R., Edmunds, W.M., Shearer, T.R., Walton, N.R.G., Jacovides, J., 1980. Assessment of recharge to aquifers. Hydrological Sciences—Bulletin des Sciences Hydrologiques 25/3/9, 217–235.
- Kypris, D.C., 1995. Diachronic changes of rainfall and the water resources in Cyprus. In: Tsiouris, N., (Ed.), Water Resources Management Under Drought or Water Shortage Conditions, Balkema, Rotterdam, pp. 11–18.
- Lindsey, B.D., Loper, C.A., Robert, A., Hainly, R.A., 1997. Nitrate in ground water and stream base flow in the lower Susquehanna river basin, Pennsylvania and Maryland. Water-Resources Investigations Report 97-4146. US Geological Survey, p. 78.
- Linsley, R.K., Kohler, M.A., Paulhus, J.L., 1982. Hydrology for engineers, Third Ed., McGraw-Hill, New York, pp. 210–212.
- Maloszewski, P., Zuber, A., 1982. Determining the turnover time of groundwater systems with the aid of environmental tracers. I. Models and their applicability. Journal of Hydrology 57, 207–231.
- Malpas, J., Moores, E.M., Panayiotou, A., Xenophontos, C. (Eds.), 1990. Ophiolites. Oceanic Crustal Analogues, Proceeding of the 'Troodos 87' Symposium, Cyprus Geological Survey, Nicosia.
- Nathan, R.J., McMahon, T.A., 1990. Evaluation of automated techniques for base flow and recession analyses. Water Resources Research 26, 1465–1473.
- NRC (National Research Council), 1996. Rock fractures and fluid flow, National Academy Press, Washington DC.
- Ofterdinger, U.S., Renard, Ph., Loew, S., 2003. Hydraulic subsurface measurements and hydrodynamic modeling as indicators for groundwater flow systems in the Rotondo granite, Submitted for publication.
- Omorpos, C., Kambanellas, C.A., Hadjigeorgiou Savvidou, P., Selipa, S., Andrew, P., Ioannou, I., 1996. Water development in Cyprus. Technical Report. Press and Information Office, Republic of Cyprus, p. 6.
- Pettyjohn, W.A., Henning, R., 1979. Preliminary estimate of ground-water recharge rates, related streamflow and water quality in Ohio. Project Completion Report 553, Technical Report, Columbus, Ohio State University, Water Resources Centre, 323 p.
- Schmidt, G., Avraamides, C., Plothner, D., Wagner, W., Zomenis, S., 1988. Technical cooperation Cyprus-German Geological and Pedological Project, Groundwater Model Investigation on the Kiti Aquifer. Bundestanstalt für Geowissenschaften und Rohstoffe, Hanover.
- Sindalovski, L., 1999. Computer program support of the trial operation test on contaminated site, PhD Thesis (in Russian). St. Petersburg State Mining Institute (Technical University), pp. 40–137.
- Sinclair, K.A., Pitz, C.F., 1999. Estimated baseflow characteristics of selected Washington rivers and streams. Water Supply Bulletin No. 60, Washington State Department of Ecology, Publication No. 99-327, Olympia, Washington, 221 p.
- Sloto, R.A., Crouse, M.Y., 1996. HYSEP: a computer program for streamflow hydrograph separation and analysis. Water-Resources Investigations Report 96-4040. US Geological Survey, Lemoyne, Pennsylvania, pp. 1–7.
- Stern, R., Knock, J., Hack, H., 1991. Instat PC Climatic Guide, Technical Report. Statistical Services, University of Reading, Reading, UK.
- Stichler, W., Maloszewski, P., Moser, H., 1986. Modelling of river water infiltration using oxygen-18 data. Journal of Hydrology 83, 355–365.
- Varga, R., Gee, J.S., Bettison-Varga, L., Anderson, R.S., Johnson, C.L., 1999. Early establishment of seafloor hydrothermal systems during structural extension: paleomagnetic evidence from the Troodos ophiolite Cyprus. Earth and Planetary Science Letters 171 (2), 221–235.
- Verhagen, B.T., Geyh, M.A., Fröhlich, K., With, K., 1991. The Lefkara area, Cyprus. In Isotope hydrological methods for the quantitative evaluation of ground water resources in arid and semi-arid areas. Research Reports of the Federal Ministry for Economic Cooperation of the Federal Republic of Germany, Bonn, Germany, pp. 43–59.